

Published in final edited form as:

*Biomaterials*. 2015 May ; 51: 250–256. doi:10.1016/j.biomaterials.2015.02.013.

# A plug-and-play ratiometric pH-sensing nanoprobe for high-throughput investigation of endosomal escape

**Zhou J. Deng**[#a], **Stephen W. Morton**[#a], **Daniel K. Bonner**[a], **Li Gu**[a], **Hooisweng Ow**[b], and **Paula T. Hammond**[*,a]

[a] Chemical Engineering, Koch Institute for Integrative Cancer Research Institute for Soldier Nanotechnologies Massachusetts Institute of Technology

[b] Ow Aramco Research Center Boston, MA

[#] These authors contributed equally to this work.

## Abstract

An important aspect in the design of nanomaterials for delivery is an understanding of its uptake and ultimate release to the cytosol of target cells. Real-time chemical sensing using a nanoparticle-based platform affords exquisite insight into the trafficking of materials and their cargo into cells. This versatile and tunable technology provides a powerful tool to probe the mechanism of cellular entry and cytosolic delivery of a variety of materials, allowing for a simple and convenient means to screen materials towards efficient delivery of therapeutics such as nucleic acids.

### Keywords

nanoparticle; endosomal escape; chemical sensing; delivery; nanotechnology

## 1. Introduction

Chemical sensing at a molecular level is fundamentally important to understanding the mechanisms governing a number of processes, including those of biological interest such as cell uptake, gene transfection, and tumor development and maturation [1-6]. A number of materials, including quantum dots [7], nanocrystals [8], and polymeric nanoparticles [9, 10] have been developed for these purposes, using fluorescence as a means of probing cellular processes. These platforms have proven to be robust, highly fluorescent tags for labeling cellular compartments to facilitate studies utilizing fluorescence microscopy, as well as stable *in vivo* imaging systems.



[*] Corresponding Author: hammond@mit.edu.

Designing systems that can molecularly recognize and identify targets, or respond to the local environment, is an attractive “nanoparticle laboratory” concept – one that is being further developed with core-shell silica nanoparticle technology [11-13]. The purpose of these systems is to facilitate continued development of biomaterials for applications such as bioimaging or therapeutic delivery. Incorporation of these plug-and-play technologies offers useful insight into the trafficking of biomaterials in cells. Of particular interest to the community are more efficient modes of cytosolic delivery for therapeutics, such as nucleic acids, that require safe passage through endosomal/lysosomal compartments for biological effect [14-17].

Currently, the most common techniques used to assess endosomal escape use confocal microscopy [18-23]. In this approach, the biomaterial, the therapeutic and the intracellular organelles, such as endosomes and lysosomes, are directly labeled with fluorescent dyes, and endosomal escape is visually evaluated based on the temporal and spatial localization of fluorescence inside cells. While this does allow for direct visualization of the processes in question, this is a low-throughput, largely qualitative technique. What is currently lacking is the ability to easily perform a quantitative, high-throughput assay with commonly available equipment and techniques without the need to directly modify the cargo to be delivered. Here, we report the development of an easily adaptable assay for quantitative and high-throughput evaluation of endosomal escape. This was achieved through deployment of a ratiometric pH-sensing nanoprobe for real-time intracellular tracking of materials.

## 2. Materials and methods

### 2.1. Materials

GFP-expressing plasmid DNA was purchased from Invitrogen. PLL (15 kDa and 50 kDa), poly-L-arginine (15 kDa and 50 kDa), poly-L-histidine (15 kDa), chitosan (15 kDa), linear PEI (2.5 kDa and 25 kDa) and branched PEI (25 kDa) were purchased from Sigma-Aldrich. Lipofectamine 2000 was purchased from Invitrogen. CCK-8 cell proliferation assay kit was purchased from Sigma-Aldrich. Human cancerous cell lines, including BT-20, A549, and MDAMB-468 were purchased from ATCC and grown according to ATCC protocols. All cell culture media and reagents were purchased from Invitrogen. PLL, poly-L-arginine and PEI were dissolved in saline buffer at pH 7.4, containing 150 mM NaCl and 10 mM phosphate; whereas poly-L-histidine and chitosan were dissolved in saline buffer at pH 5.5, containing 150 mM NaCl and 10 mM acetate. Ultrapure water (18.2 MΩ•cm) was generated with a Barnstead Nanopure water purification system. Absolute ethanol, ammonium hydroxide solution and Sodium hydroxide (NaOH, 98.0+%) were purchased from Fluka. 3-(triethoxysilyl)propyl isocyanate, 70kDa poly-L-lysine, hydrochloric acid (HCl, 37%) and Orange II sodium salt (98.0+%) were purchased from Sigma-Aldrich. Atto647 succinimidyl ester was purchased from Atto Tec GmbH, Germany. 5(6)-Carboxyfluorescein, succinimidyl ester was purchased from Anaspec. Aminopropyltriethoxysilane (95%), PEG-silane (95%) and tetraethylorthosilicate (99%) were purchased from Gelest. pH of dye solution was measured on an Accumet Excel XL15 pH/mV/Temperature meter. Absorbance of solutions was recorded on a Varian Cary 5000 UV-Vis-NIR spectrophotometer.

### 2.2. Synthesis of core-shell silica nanoparticles

The core-shell silica nanoparticles were synthesized according to the previously established method [9] (Supporting Figure 1). Briefly, the reference dye, Atto647 succinimidyl ester was conjugated to the silica precursor aminopropyltriethoxysilane in an anhydrous nitrogen environment. This conjugate was then hydrolyzed in basic ethanolic solution with a pure silica precursor, tetraethylorthosilicate, catalyzed by concentrated aqueous ammonia. After the synthesis of these particles containing the reference dyes, the sensor dye, fluorescein (FITC), in the form of fluorescein succinimidyl ester, was conjugated with 3-aminopropyltriethoxysilane under similar conditions. The sensor dye precursor was then hydrolyzed with further tetraethyl orthosilicate to form the sensor layer. Following synthesis, the particles were centrifuged and resuspended repeatedly in ethanol and finally deionized water. We functionalized the surface of the pH sensor particles with a molar mixture of 95:5 PEG-silane and Poly-L-lysine where the latter was first silanized with 3-(triethoxysilyl)propyl isocyanate. The functionalized pH sensor particles were purified via centrifugation washes using 100k MWCO spin filters to remove unbound PEG or poly-L-lysine.

### 2.3. Nanoparticle characterization

Primary amine groups from poly-L-lysine conjugated to pH sensor particles' surface were quantified by Orange II method reported by Noel *et. al.* [24]. One milligram pH sensor particles was immersed in 1.5 mL of dye solution (14 mg/mL) in acidic solution (pH = 3) for 30 min at 40°C. The particles were then washed thrice using the acidic solution (pH = 3) through spin filter (100 kDa MWCO) at 5000 rpm for 10 min each to remove unbound dye. The particles were air-dried and then immersed in 3 mL of alkaline solution (ultrapure water adjusted to pH 12 with a 1 M NaOH solution) for 2 hours to release the bound dye from particle surface into the solution. The pH of the solution containing the desorbed dye was adjusted to pH 3 by adding 37% HCl. The absorbance at 484nm of the solution was then measure. The concentration of primary amine group can be calculated using reported extinction coefficient of Orange II at 482 nm ($\varepsilon$ = 18,200 $M^{-1}$•$cm^{-1}$). It is estimated that 45±10 primary amine groups present on a 30 nm pH sensor particle.

### 2.4. Intracellular pH sensing assays

To assess the ability to sense pH intracellularly, silica nanoparticles were incubated with cells at different pH and cell-associated fluorescence was quantitated by flow cytometry. Briefly, cells were seeded in a 24-well plate at density of 1 X $10^5$ cells per well and grown for 24 hours. After changing into fresh the media, cells were treated with the silica nanoparticles at the concentration of 100 μg/ml for 2 hours at 37°C. At the end of incubation, free nanoparticles were washed off twice with fresh media, and the cells were trypsinized and pelleted. Cells were then resuspended in each of different cellular pH clamping buffer (pH 4, 5, 6, 6.6 and 7.4) that were made by mixing of 50 mM HEPES (pH 7.4) and 50 mM MES (pH 4.0) buffers, each containing 50 mM NaCl, 30 mM ammonium acetate and 40 mM sodium azide [25].

### 2.5. In vitro cell trafficking – flow cytometry

To screen the intracellular trafficking of gene delivery vehicles, the cells were firstly seeded in a 96-well plate at density of 2 X $10^4$ cells per well for 24 hours, and co-treated with each of the transfection agents and silica nanoparticles at various concentrations and incubation times. By the end of the incubation, cells were washed in fresh media and resuspended with trypsin. The cell-associated FITC:Atto647 fluorescent ratio was determined by flow cytometry and the ratios were converted to the average intracellular pH using a calibration curve.

### 2.6. Cell transfection

DNA-polymer complexes were firstly prepared by mixing 1 μg/ml GFP plasmid DNA with 10 μg/ml polymeric vehicles or 3 μl/ml Lipofectamine 2000 in serum-free OptiMEM for 30 minutes at room temperature. The siRNA-loaded lipid-based nanoparticles were prepared according to the previously described methods using microfluidic device. The cells, seeded in a 96-well plate at 2 X $10^4$ cells per well for 24 hours, were treated with the transfecting complexes at various concentrations. After 48 hours of incubation, the GFP expression was examined for DNA transfection or for siRNA silencing using flow cytometry.

### 2.7. Flow cytometry

Flow cytometry was performed using a FACS LSR II coupled with a high-throughput system for the 96-well plate format (BD biosciences, San Jose, CA). FITC were excited at 488 nm and detected at 530/30 nm; where Atto647 were detected at 635 nm and detected at 660/20 nm. Cells were gated by forward and side scatter and 5,000 events were collected for each sample. The geometric means of fluorescence intensities were recorded to determine the FITC:Atto647 fluorescent ratios. The cellular uptake of the silica nanoparticles were assessed using the geometric means of cell-associated Atto647 fluorescence that is insensitive to pH change.

### 2.8. Cytotoxicity assay

Cytotoxicity assays were performed in parallel with the intracellular pH sensing assays to assess the cytotoxicity of the silica nanoparticles and transfection agents. Briefly, cells were firstly seeded in a 96-well plate at density of 2 X $10^4$ cells per well for 24 hours and treated with the nanoparticles or transfection agents at various concentrations. Over different incubation times, the cells were replaced in fresh serum-free OptiMEM media containing 10% v/v of the CCK-8 proliferation reagent. After 2 hours incubation at 37°C, the absorbance at 450 nm was measured by a plate reader. Cell viabilities were normalized to an untreated control and calculated using a standard curve.

### 2.9. Confocal Microscopy

Confocal microscopic images were taken using a Nikon A1R Ultra-Fast Spectral Scanning Confocal Microscope (Nikon instruments Inc., Melville, NY). Cells were seeded in CELLview glass bottom dish (Greiner Bio-One GmbH, Germany) at 1 x $10^5$ cells per well and grown overnight. Cells were treated with 3 μg/ml of branched PEI or 3 μl of Lipofectamine 2000 in the presence of 100 μg/ml nanoparticles, or with 100 μg/ml

nanoparticles along for 4 hours. Cells were then washed three times and stained with DAPI for 15 minutes at 37°C, followed by three more washes and microscopic imaging at DAPI, FITC and Atto647 channels.

### 2.10. Statistical Analysis

Experiments were performed in triplicates, or otherwise indicated. Data were analyzed using descriptive statistics, single-factor analysis of variance (ANOVA), and presented as mean values ± standard deviation (SD) from three to eight independent measurements. Statistical comparisons between different treatments were assessed by two-tailed t tests or one-way ANOVA assuming significance at $p$-value < 0.05.

## 3. Results and Discussion

The ratiometric pH-sensing nanoprobes were developed based on a core-shell silica nanoparticle architecture, and were synthesized via a modified Stöber method whereby a reference dye was covalently bound within the silica core initially, followed by deposition of a sensor dye-containing silica layer on the surface [12, 13] (Supporting Figure 1). The exterior silica layer can be further modified with silane-functionalized ligands through the surface tetraethyl orthosilicate [13]. Herein, nanoprobes of 30 ± 2.6 nm in diameter were specifically synthesized (Supporting Figure 2A). The nanoparticles were modified with a molar mixture of 95:5 polyethylene glycol(PEG)-silane and silanized poly-L-lysine (PLL) to create a slightly positively charged surface with a zeta potential of 5 ± 1.2 mV when measured in PBS at pH 7.4 (Supporting Figure 2B). The nanoparticles were uniform spheres (Figure 1A and Supporting Figure 2C) with a polydispersity index of 0.13. A pH-insensitive reference dye, Atto647, was covalently incorporated deep within the organosilica core during particle synthesis and is thus protected from the environmental fluctuations; while a sensor dye precursor of 3-aminopropyltriethoxysilane conjugated with a pH-responsive dye, FITC, through its succinimidyl ester, was then hydrolyzed with further tetraethyl orthosilicate to form the sensor layer. This architecture ensures that changes in environmental pH only affect the sensor fluorescence (Figure 1B). It was found that the FITC:Atto647 fluorescence ratio was highly correlated with the change in pH over a range of 4 to 7.5 (Supporting Figure 3A). This ratiometric change could be detected in real-time by fluorescence, and was found to be reversible when switched between different pH environments (Supporting Figure 3B). In addition, these nanoprobes retained their pH-dependent fluorescent ratiometric property (Figure 1C) as well as their hydrodynamic size (hydrodynamic light scattering, Figure 1D) in tissue culture medium (10% serum proteins) for at least 24 hours. These features allow the nanoprobes to dynamically sense the pH within a physiologically relevant environment over a prolonged period of time; the ratiometric nature of the nanoparticles allows the pH data to be measured independent of the extent of cell uptake and the nature of the targeting moiety, among other features of the nanoparticle design.

We first assessed the feasibility of using these nanoprobes for intracellular pH sensing. In human triple-negative breast cancer cells, BT-20, we observed concentration-dependent uptake of the nanoprobes as determined by the cell-associated Atto647 fluorescence intensity via flow cytometry (Supporting Figure 4A). A MTT-derived cytotoxicity assay

performed with BT-20 cells indicated that the nanoprobes were non-cytotoxic even at concentrations up to 1.5 mg/ml over 48 hours (Supporting Figure 4B). The results indicated that these nanoprobes were biocompatible while promoting cellular internalization. Next, BT-20 cells were treated with 100 μg/ml nanoprobes for 2 hours at 37°C to allow maximal internalization, followed by washes and exposure to a series of pH-clamping buffers between pH 4 to 7.4. The buffer contained 40 mM sodium azide to inhibit cellular respiration and clamp the intracellular pH at the pre-adjusted value [26]. Using flow cytometry, the expected correlation between the change in FITC:Atto647 cell-associated fluorescence ratio and the intracellular pH was observed. This was evidenced by a parallel right shift of the cell population along the FITC axis on the FITC/Atto647 scatter plot (Figure 1E). A calibration curve of the ratiometric output of the nanoprobe fluorescence against the intracellular pH was generated using a cubic polynomial model based on the best fit [13], producing an $R^2$ value of 0.9887 (Figure 1F). From here, we were able to use these nanoprobes to determine the pH in their intracellular environment.

We next tested whether this capability would allow us to monitor real-time intracellular trafficking. In BT-20 cells treated with the nanoprobes, the environmental pH of the nanoprobes dropped from pH 7.4 to 4 over the first 2 hours (Figure 2A). This suggested a rapid cellular internalization process of the nanoprobes through endocytosis, followed by acidification within endolysosomes. The pH remained at around 4 for 24 hours, indicating the inability of the nanoprobes alone to escape from the acidic vesicles. Endosomal entrapment is a natural mechanism that protects the cytoplasmic content from interacting with potentially harmful exterior materials, and it is one of the major hurdles for designing efficient cytosolic delivery of cargo, such as nucleic acids, requiring such access for biological effect [17, 27]. To further confirm that the nanoprobes were indeed trapped in the endolysosomes, we co-treated the cells with the nanoprobes and 1 μg/ml 25 kDa branched polyethylenimine (PEI). PEI, a highly cationic polyelectrolyte, contains functional secondary and tertiary amines that have been known to mediate endosomal escape through a so-called proton sponge effect [28], and it has been used as the gold standard among off-the-shelf polymeric materials for *in vitro* nucleic acid delivery. The PEI co-treatment not only prevented a complete acidification by retaining the pH at 5.5 in the first few hours, but also reversed the pH to 7.4 at 24 hours post-incubation (Figure 2A), potentially by mediating the endosomal escape of the nanoprobes. In contrast, co-treatment of 1 μg/ml 15 kDa PLL failed to prevent the complete acidification or to mediate the escape (Figure 2A). This was consistent with the perception that PLL has low transfection efficiency due to its lack of secondary or tertiary amines [29, 30]. However, further addition of 10 μM chloroquine, a weak base that is able to buffer acidic cellular vesicles [26], was able to retain the pH above 4 over a period of 24 hours (Figure 2A). The data again confirmed that the nanoprobes were capable of dynamically sensing the subtle changes of pH in the intracellular environment, and this property can be used to precisely and quantitatively validate endosomal escape.

None of the above treatments appeared cytotoxic based on a MTT-derived cytotoxicity assay (Supporting Figure 5), ruling out the possibility of cell death-induced intracellular pH change. Moreover, similar results were obtained in different cell lines, including the triple-negative BT-20 and MDA-MB-468 cells and the non-small lung cancer A549 cells

(Supporting Figure 6), suggesting the generalizability of this platform technology for intracellular pH sensing.

Endosomal escape is central to successful intracellular delivery of biomaterials and therapeutics, such as nucleic acids. The capability of these nanoprobes to quantitatively measure endosomal escape may allow us to better understand the role of escape on the transfection efficiencies of newly synthesized delivery systems. Thus, we evaluated a library of polymeric carriers previously evaluated for nucleic acid delivery, including 15 kDa and 50 kDa PLL, 15 kDa and 50 kDa poly-L-arginine, 15 kDa poly-L-histidine, 15 kDa chitosan, 2.5 kDa and 25 kDa linear PEI, and 25 kDa branched PEI. A green fluorescence protein (GFP)- expressing DNA plasmid was deployed to complex with each carrier and to transfect BT-20 cells. Briefly, cells were co-treated with 100 μg/ml of the nanoprobes and 10 μg/ml of the DNA-loaded carrier. Two hours post-incubation, the intracellular pH of the nanoprobes was determined (Figure 3A, upper panel). In a parallel study without the nanoprobe co-treatments, the transfection efficiencies were examined by the fluorescent intensity of GFP in cells 48 hours post-incubation (Figure 3A, lower panel). A significant positive correlation was observed between the intracellular pH and the GFP intensity with a *p*-value of 0.0008 and a $R^2$ value of 0.77 (Figure 3B). Among the selected carriers, the PEI family achieved the highest GFP transfection, which correlated with an intracellular nanoprobe pH of 7. In contrast, the DNA only, 15 kDa chitosan and 15 kDa poly-L-histidine treatments were associated with a low intracellular nanoprobe pH of 4.2 and no detectable GFP expression. Some of the polymeric materials, such as chitosan and poly-L-histidine, exhibited little transfection efficiency in this screening despite their reportedly high transfection efficiency. Differences here can be attributed to the transfection conditions, such as DNA-binding solutions, pH and N:P ratios, which were not optimized for each polymer but rather standardized across a range of materials for general investigation of endosomal escape. Nevertheless, the data reported herein indicate a correlation between the degree of endosomal escape and the levels of target gene expression, which is consistent with previous work [31]. The high-molecular weight PLL, PLA, and linear PEI exhibited higher intracellular pH and higher transfection efficiencies than their lower molecular-weight counterparts, suggesting that molecular weight might play a role in endosomal escape, consistent with previous reports [32]. In addition, the intracellular nanoprobe pH was dependent on the polyplex concentrations (Supporting Figure 7). An increase in the concentration of, for example, the 2.5 kDa LPEI-DNA polyplex from 3 μg/ml to 10 μg/ml in BT-20 cell treatments resulted in the intracellular nanoprobe pH increase from 5 to 6, which corresponded to an increase in GFP expression level from 600 relative fluorescent units (RFU) to 1750 RFU. Together, these results suggest that the intracellular pH is an effective index of endosomal escape and can be used to predict the transfection efficiencies of polymeric carriers – all by co-administration of the material system of interest with the ratiometric silica bead technology as a non-invasive, label-free approach to probe cellular trafficking. Our study provides strong evidence that the pH measured by silica nanoparticles is highly correlated with endosomal escape, which is estimated as the outcomes of DNA transfection or siRNA silencing.

Besides the polymeric materials, cationic lipid-based materials are another common type of non-viral carrier for nucleic acid delivery. We first deployed the commercially available lipofectamine® reagent to investigate this type of carrier. Surprisingly, the nanoprobes reported a low level of endosomal escape, albeit a high level of target protein expression was observed (Figure 2A, Supporting Figure 8). The result implied that the nanoprobes were not able to co-traffic with the DNA out of the endosomes. We further confirmed this discrepancy by confocal microscopy (Figure 2B). The lipofectamine co-treatment resulted in a punctate pattern of nanoprobes across the cytoplasm, similar to that of the nanoprobe-only treatment, indicative of endosomal entrapment. In contrast, the nanoprobes co-treated with the branched PEI were located throughout the cytoplasm. To further investigate the lipid-based carriers, we screened a lipid-based nanoparticle (LNP) (courtesy of Professor Chris Alabi of Cornell University) that was optimally designed for high efficiency siRNA delivery [27, 33]. Again, we saw that the siRNA-loaded LNP significantly silenced the target gene in the tested cells, but the nanoprobes reported a low pH of 4 (Supporting Figure 9). Together, the data implied a mechanistic difference in endosomal escape between the polymer-based and the lipid-based nucleic acid carriers. In a recent study, Rehman *et al*. [21] using confocal microscopy, showed that polymer-based systems were associated with a rapid and simultaneous release of both the nucleic acid cargo and the polymer carrier from the endosomal compartment, while the lipid-based system displayed a gradual release over extended periods of time in a fashion that only allows the nucleic acid to be released into the cytoplasm, but the lipid carrier remained associated with the endosomes. This study is consistent with our findings, which proposes that the polymers cause rigorous destabilization of the endosomal membrane and result in simultaneous and immediate release of all the contents; while the lipids induce more subtle changes in membrane integrity following fusion and subsequently a “leakage-like” release of the nucleic acids. Based on the data, the 30 nm nanoprobes, however, were not able to leak through the lipid-induced compromised membrane. The size exclusion might be one of the possible explanations for such drastic differences in elucidating transfection efficiency of polymer- versus lipid-based material delivery systems.

The mechanism of endosomal escape for different materials depends on the system's chemical composition, interactions with intracellular components, and release rates of cargos [27]. Despite recent progress, our understanding of this complex and multivariate process is lacking and far from comprehensive [34]. In an earlier work [26], the researchers tracked endosomal escape events through chemical conjugation of fluorescent dyes directly to the pDNA molecules to be delivered. Although this method is able to measure the change of the pDNA pH environment, it is not clear whether the chemical modification changes the intracellular behavior of the tested pDNA. Further, this method is limited to DNA tracking; while investigation of other types of materials, such as RNA or proteins, requires completely different chemistry strategies. In comparison, the approach reported here aims to develop an easy-to-use tool that can be widely applied for investigation of a broad range of biomaterials. Instead of chemically modifying the material of interest, we deployed a nanoprobe that co-traffics with the material and provides a quantitative readout of their intracellular behavior. Here, we report the capability of investigating not only transfection of pDNAs, but also gene silencing of siRNAs. Our assay also has the potential to study

proteins or synthetic nanoparticles, which often lack effective chemical handles for fluorescent dye conjugations. These pH-sensing nanoprobes provide a versatile research platform for interrogating the endocytic paths of various materials. First, the dyes are deeply and covalently encapsulated in the nanoprobes, effectively retaining their stability, sensitivity, and pH-responsiveness in various cellular environments. Second, the core-shell architecture allows the size to be tuned from tens of nanometers to several microns in scale while providing a biocompatible and easily functionalized outer surface for mediating cellular entry and mimicking functional nanomaterials of interest for investigation [35]. Here, we used PLL/PEG blend surface for the nanoprobes to facilitate cell membrane binding. It is possible that the positive charge on the nanoparticles interacts with negatively charged pDNA during the intracellular trafficking. However, we have demonstrated that PLL/PEG-coated nanoparticles were inert for endosomal escape (Figure 2) or gene transfection (Figure 3), indicating that our silica nanoprobes do not alter the intracellular behavior of the DNA/polymer complexes of interests. Moreover, we demonstrated that nanoprobes could be made with stealth, cell binding, or cell penetrating properties (via a functionalized silane derivative, e.g. isocyanate for PLL immobilization) when functionalized with a combination of macromolecules, including PEG, PLL, and TAT oligopeptides - a cell penetrating peptide that facilitates endosomal escape (Supporting Figure 10) [36]. Such flexibility in design affords customization of the nanoprobes, unlike small molecular dyes, in a built-to-order fashion to achieve desired biological interactions with proteins, lipids, nucleic acids, and other cellular organelles. A library of nanoprobes with various size, charge, hydrophobicity, and surface properties can be deployed for systematic investigations of endosomal escape.

In this work, we have developed an easy-to-use and high throughput assay for quantitatively evaluating intracellular delivery, specifically for nucleic acid delivery of polymeric carriers. The nanoprobes are deployed in a “plug-and-play” fashion as a non-interfering and biocompatible co-treatment with the tested materials. Our method does not provide direct information on cellular uptake; rather, it provides the eventual outcomes resulting from the combination of cellular uptake, endocytosis, and endosomal escape. These nanoparticles are a tunable platform to probe the cellular trafficking of material systems being tested. In doing so, the ratiometric silica beads temporally resolve the change in local pH environment of the materials of interest, providing a convenient, quantitative readout of their ability to mediate endosomal escape. This approach relies on customizing the physicochemical characteristics (size, surface properties) of the probes to fit the material system of interest so as to allow them to traffic together following co-administration. Since the labeling on tested materials is not required, this assay can be applied to various materials without further modification or labeling, such as nucleic acids, proteins, synthetic polymers, and inorganic materials.

In this study, we demonstrated the effectiveness of using these nanoprobes for evaluating the transfection efficiency of nucleic acids. In contrast to directly measuring the change in gene expression with a typical turnover period of 48-72 hours, the current assay is adapted to monitor endosomal escape – a key step for the intracellular delivery process – thus greatly shortening the time of the experiment to 2 hours. The assay can be easily scaled up for high throughput screening, which is more advantageous than the current confocal microscopic techniques [18]. Moreover, the quantitative nature of this assay allows efficient screening of

key physicochemical parameters involved in the intracellular delivery of new materials. In the current work, the screening of the selected polymer carriers has revealed important factors that are known to be associated with transfection efficiency, including molecular weight, amine chemistry, polymer structure, and pKa. We have developed an assay that is of great value to the discovery of novel intracellular delivery carriers.

## 4. Conclusion

We have demonstrated a powerful application of ratiometric pH-sensing nanoprobes for real-time intracellular pH quantitation – critical towards the development of the next generation of drug delivery systems. Using these nanoprobes, an assay with the "plug-and-play" concept has been developed to evaluate transfection efficiencies of polymeric carriers for nucleic acid delivery. Easy application with no need for labeling of tested materials, this assay allows for rapid, quantitative screening of a library of new material delivery systems. Further development of this simple tool can be useful for assays in which the pH of intracellular environments is of interest, including environmental sensing, intracellular trafficking studies, and the delivery of nucleic acids, proteins, and other macromolecular agents.

## Supplementary Material

Refer to Web version on PubMed Central for supplementary material.

## Acknowledgements

The authors would like to thank funding for providing valuable resources to facilitate this work. These include grants from the Center for Cancer Nanotechnology Excellence (CCNE), grant number: 5 U54 CA151884-02, and the Koch Institute Nanoparticle Grant. The authors would like to acknowledge the team at Hybrid Silica Technologies (HST), specifically Yaqi Wang, Kenneth Wang, and Yuefei Gong, for fabrication and delivery of nanoparticle systems for testing, as well as discussion of experimental details and results. The authors would also like to further acknowledge the Koch Institute for Integrative Cancer Research at MIT for providing resources central to the completion of this work – specifically, the Koch Institute Swanson Biotechnology Center core facilities (microscopy, flow cytometry) for facilitating biological data, as well as the Peterson (1957) Nanotechnology core (Dr. Yun, cryogenic-transmission electron microscopy) – all supported by the Koch Institute Core Grant P30-CA14051 from the NCI. S.W.M. would like to acknowledge funding from the National Science Foundation Graduate Research Fellowship (N.S.F. G.R.F.P.). Z.J.D. would like to acknowledge a fellowship funding from the National Health and Medical Research Council, Australia. Hooisweng Ow now works for Aramco Research Center in Boston, MA.

## References

1. Voura E, Jaiswal J, Mattoussi H, Simon S. Tracking metastatic tumor cell extravasation with quantum dot nanocrystals and fluorescence emission-scanning microscopy. Nat Med. 2004; 10:993–8. [PubMed: 15334072]
2. Mattoussi H, Palui G, Na HB. Luminescent quantum dots as platforms for probing in vitro and in vivo biological processes. Adv Drug Deliver Rev. 2012; 64:138–66.
3. Saha K, Agasti SS, Kim C, Li XN, Rotello VM. Gold Nanoparticles in Chemical and Biological Sensing. Chem Rev. 2012; 112:2739–79. [PubMed: 22295941]
4. Zrazhevskiy P, Sena M, Gao XH. Designing multifunctional quantum dots for bioimaging, detection, and drug delivery. Chem Soc Rev. 2010; 39:4326–54. [PubMed: 20697629]
5. Gu L, Faig A, Abdelhamid D, Uhrich K. Sugar-based amphiphilic polymers for biomedical applications: from nanocarriers to therapeutics. Accounts Chem Res. 2014; 47:2867–77.

6. Gu L, Nusblat LM, Tishbi N, Noble SC, Pinson CM, Mintzer E, et al. Cationic amphiphilic macromolecule (CAM)-lipid complexes for efficient siRNA gene silencing. J Control Release. 2014; 184:28–35. [PubMed: 24727076]
7. Dennis AM, Rhee WJ, Sotto D, Dublin SN, Bao G. Quantum Dot-Fluorescent Protein FRET Probes for Sensing Intracellular pH. ACS Nano. 2012; 6:2917–24. [PubMed: 22443420]
8. Somers RC, Lanning RM, Snee PT, Greytak AB, Jain RK, Bawendi MG, et al. A nanocrystal-based ratiometric pH sensor for natural pH ranges. Chem Sci. 2012; 3:2980–5.
9. Sun HH, Almdal K, Andresen TL. Expanding the dynamic measurement range for polymeric nanoparticle pH sensors. Chem Commun. 2011; 47:5268–70.
10. York AW, Zablocki KR, Lewis DR, Gu L, Uhrich KE, Prud'homme RK, et al. Kinetically assembled nanoparticles of bioactive macromolecules exhibit enhanced stability and cell- targeted biological efficacy. Adv Mater. 2012; 24:733–9. [PubMed: 22223224]
11. Lapresta-Fernandez A, Doussineau T, Dutz S, Steiniger F, Moro AJ, Mohr GJ. Magnetic and fluorescent core-shell nanoparticles for ratiometric pH sensing. Nanotechnology. 2011:22.
12. Ow H, Larson DR, Srivastava M, Baird BA, Webb WW, Wiesner U. Bright and stable core- shell fluorescent silica nanoparticles. Nano Lett. 2005; 5:113–7. [PubMed: 15792423]
13. Burns A, Sengupta P, Zedayko T, Baird B, Wiesner U. Core/Shell fluorescent silica nanoparticles for chemical sensing: towards single-particle laboratories. Small. 2006; 2:723–6. [PubMed: 17193111]
14. Pichon C, Billiet L, Midoux P. Chemical vectors for gene delivery: uptake and intracellular trafficking. Curr Opin Biotechnol. 2010; 21:640–5. [PubMed: 20674331]
15. Zhao F, Zhao Y, Liu Y, Chang X, Chen C. Cellular uptake, intracellular trafficking, and cytotoxicity of nanomaterials. Small. 2011; 7:1322–37. [PubMed: 21520409]
16. Varkouhi AK, Scholte M, Storm G, Haisma HJ. Endosomal escape pathways for delivery of biologicals. J Control Release. 2011; 151:220–8. [PubMed: 21078351]
17. Whitehead KA, Langer R, Anderson DG. Knocking down barriers: advances in siRNA delivery. Nat Rev Drug Discov. 2009; 8:129–38. [PubMed: 19180106]
18. Bonner DK, Leung C, Chen-Liang J, Chingozha L, Langer R, Hammond PT. Intracellular trafficking of polyamidoamine-poly(ethylene glycol) block copolymers in DNA delivery. Bioconjug Chem. 2011; 22:1519–25. [PubMed: 21761838]
19. Sahay G, Querbes W, Alabi C, Eltoukhy A, Sarkar S, Zurenko C, et al. Efficiency of siRNA delivery by lipid nanoparticles is limited by endocytic recycling. Nat Biotechnol. 2013; 31:653–8. [PubMed: 23792629]
20. Gilleron J, Querbes W, Zeigerer A, Borodovsky A, Marsico G, Schubert U, et al. Image- based analysis of lipid nanoparticle-mediated siRNA delivery, intracellular trafficking and endosomal escape. Nat Biotechnol. 2013; 31:638–46. [PubMed: 23792630]
21. Rehman ZU, Hoekstra D, Zuhorn IS. Mechanism of Polyplex- and Lipoplex-Mediated Delivery of Nucleic Acids: Real-Time Visualization of Transient Membrane Destabilization without Endosomal Lysis. ACS Nano. 2013; 7:3767–77. [PubMed: 23597090]
22. Gu L, Zablocki K, Lavelle L, Bodnar S, Halperin F, Harper I, et al. Impact of ionizing radiation on physicochemical and biological properties of an amphiphilic macromolecule. Polym Degrad Stabil. 2012; 97:1686–9.
23. Hehir S, Plourde NM, Gu L, Poree DE, Welsh WJ, Moghe PV, et al. Carbohydrate composition of amphiphilic macromolecules influences physicochemical properties and binding to atherogenic scavenger receptor A. Acta Biomater. 2012; 8:3956–62. [PubMed: 22835678]
24. Noel S, Liberelle B, Robitaille L, De Crescenzo G. Quantification of primary amine groups available for subsequent biofunctionalization of polymer surfaces. Bioconjug Chem. 2011; 22:1690–9. [PubMed: 21736371]
25. Bayer N, Schober D, Prchla E, Murphy RF, Blaas D, Fuchs R. Effect of bafilomycin A1 and nocodazole on endocytic transport in HeLa cells: Implications for viral uncoating and infection. J Virol. 1998; 72:9645–55. [PubMed: 9811698]
26. Akinc A, Langer R. Measuring the pH environment of DNA delivered using nonviral vectors: implications for lysosomal trafficking. Biotechnol Bioeng. 2002; 78:503–8. [PubMed: 12115119]

27. Whitehead KA, Sahay G, Li GZ, Love KT, Alabi CA, Ma M, et al. Synergistic silencing: combinations of lipid-like materials for efficacious siRNA delivery. Mol Ther. 2011; 19:1688–94. [PubMed: 21750531]
28. Behr JP. The proton sponge: A trick to enter cells the viruses did not exploit. Chimia. 1997; 51:34–6.
29. Pollard H, Remy J, Loussouarn G, Demolombe S, Behr JP, Escande D. Polyethylenimine but not cationic lipids promotes transgene delivery to the nucleus in mammalian cells. J Biol Chem. 1998; 273:7507–11. [PubMed: 9516451]
30. Boussif O, Lezoualc'h F, Zanta MA, Mergny MD, Scherman D, Demeneix B, Behr JP. A versatile vector for gene and oligonucleotide transfer into cells in culture and in vivo: polyethylenimine. Proc Natl Acad Sci U S A. 1995; 92(16):7297–301. [PubMed: 7638184]
31. Varkouhi AK, Scholte M, Storm G, Haisma HJ. Endosomal escape pathways for delivery of biologicals. J Control Release. 2011; 151:220–8. [PubMed: 21078351]
32. Cai J, Yue Y, Rui D, Zhang Y, Liu S, Wu C. Effect of chain length on cytotoxicity and endocytosis of cationic polymers. Macromolecules. 2011; 44:2050–7.
33. Alabi CA, Love KT, Sahay G, Yin H, Luly KM, Langer R, et al. Multiparametric approach for the evaluation of lipid nanoparticles for siRNA delivery. Proc Natl Acad Sci U S A. 2013; 110:12881–6. [PubMed: 23882076]
34. Bonnet ME, Erbacher P, Bolcato-Bellemin AL. Systemic delivery of DNA or siRNA mediated by linear polyethylenimine (L-PEI) does not induce an inflammatory response. Pharm Res-Dord. 2008; 25:2972–82.
35. Bonnet ME, Erbacher P, Bolcato-Bellemin AL. Systemic delivery of DNA or siRNA mediated by linear polyethylenimine (L-PEI) does not induce an inflammatory response. Pharm Res-Dord. 2008; 25:2972–82.
36. Lehto T, Kurrikoff K, Langel U. Cell-penetrating peptides for the delivery of nucleic acids. Expert Opin Drug Deliv. 2012; 9:823–36. [PubMed: 22594635]

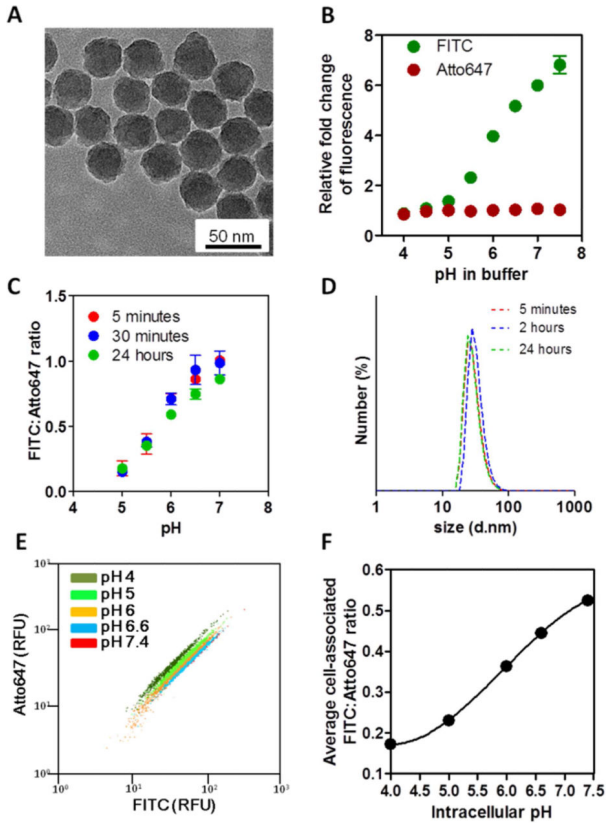


**Figure 1. Physicochemical and *in vitro* characterization of the pH-sensing nanoprobes**

**(A)** Transmission electron microscopic images of the silica nanoprobes. **(B)** Relative intensity change of FITC and Atto647 fluorescence from the nanoprobes in buffer over a range of pH conditions from 4 to 7.5 (n=3). **(C)** pH-dependent fluorescent ratiometry and **(D)** the colloidal stability of the nanoparticle fluorescence in biologically-relevant buffer over 24 hours. **(E)** Flow cytometry Atto647:FITC scatter plot of BT-20 treated with the nanoprobes in different pH-clamping buffers (n=3, representative scatter plot of each treatment is shown, RFU = relative fluorescent unit). **(F)** A pH standard curve of FITC:Atto647 against different intracellular pH (n=3).

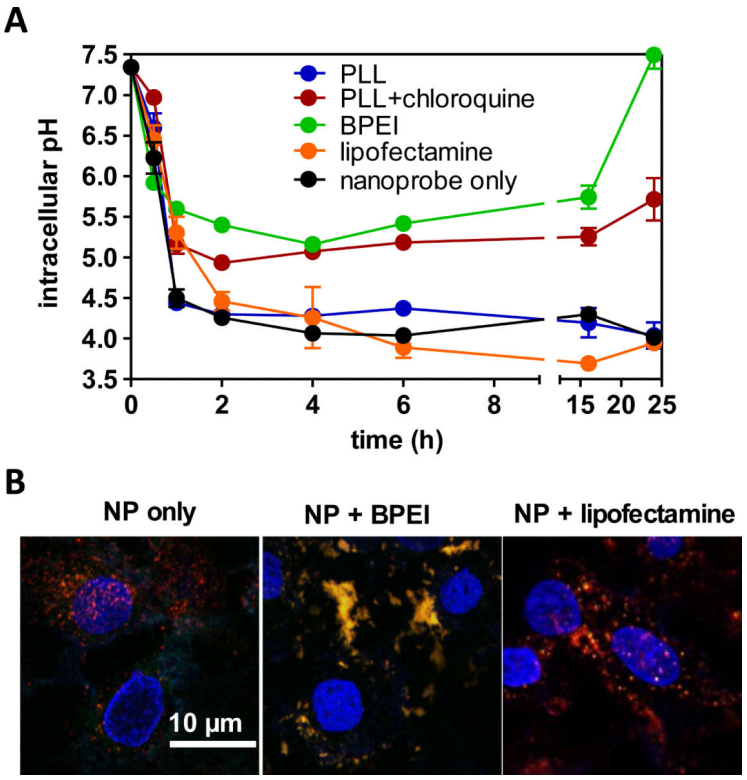


**Figure 2. Probing endosomal escape using the nanoprobes**

**(A)** Intracellular pH changes in BT-20 cells co-treated with the nanoprobes and different transfection reagents over 24 hours at 37°C (n=3, $p < 0.05$, two-way ANOVA). **(B)** Confocal microscopic images of BT-20 cells treated with the nanoprobes and BPEI or lipofectamine for 4 hours at 37°C.

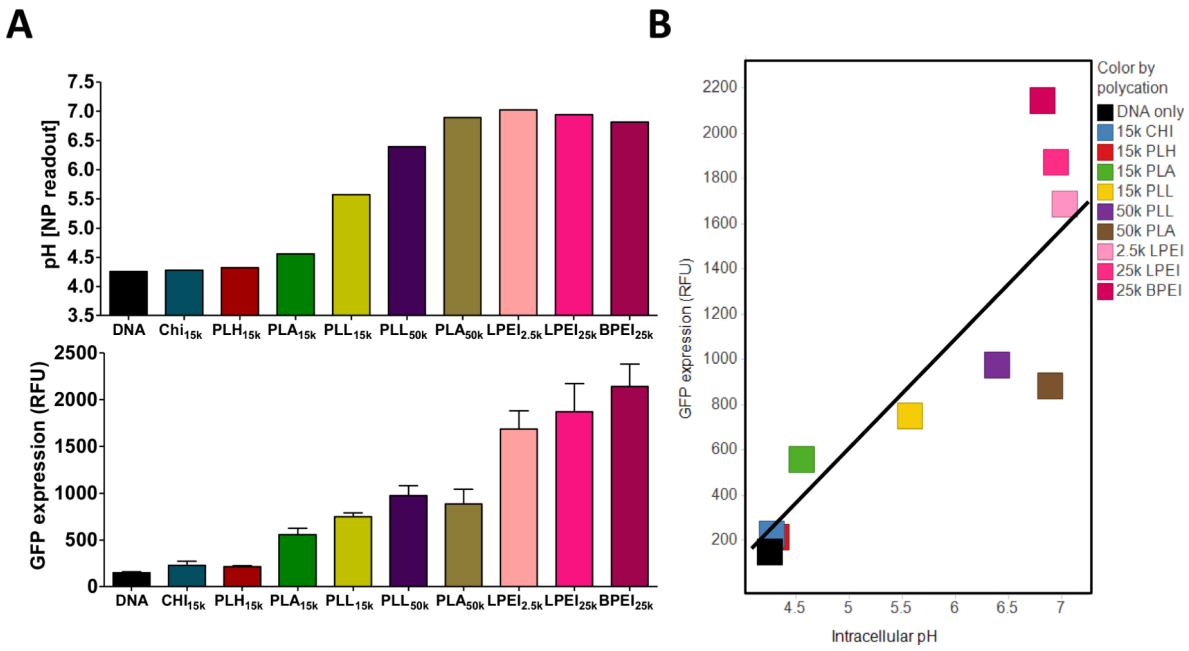


**Figure 3. Association of intracellular pH and transfection efficiency**

**(A)** Quantitative measure of average intracellular pH of the nanoprobe environment in BT-20 cells 2 hours after transfection with GFP plasmid DNA using different types of polymers (upper panel), and GFP expression of the cells 48 hours after transfection (n=3). **(B)** Correlation plot of GFP fluorescence in BT-20 cells with the intracellular pH (n=3, P < 005, $R^2 = 0.77$).